(n, n') and $(n, 2n)$ Reactions in Several Elements at 14.8 MeV†

SURESH C. MATHUR,* P. S. BUCHANAN, AND I. L. MORGAN‡
Texas Nuclear Corporation, Austin, Texas 78757
(Received 4 March 1969)

The neutron-emission cross sections for an incident neutron energy of 14.8 MeV were measured at 90° for Be, B, C, Mg, Si, Ti, V, Mn, Fe, Co, Ni, Cu, Se, Y, Mo, Cd, Sb, Ce, W, and Pb by means of a neutron time-of-flight spectrometer. The experimental data were corrected for neutron multiple scattering. From the experimental inelastic neutron distributions, the distributions for the emission of the first and second neutrons, respectively, were calculated for the medium and heavy nuclei on the basis of the statistical-model treatment of Lang and Le Couteur. The corresponding nuclear temperatures for the emission of the first and second neutrons were also obtained. The calculated inelastic distributions for the emission of the first neutrons were used to obtain the level-density parameters based on the Fermi-gas model.

I. INTRODUCTION

THE measurement of energy spectra of scattered neutrons by complex nuclei gives insight into the reaction mechanism and nuclear level densities. In the region of medium and heavy nuclei, the level densities may be considered as a continuous function of excitation energy, for excitations of a few MeV and higher. In such cases, the decay of the compound nucleus can be described by statistical models, leading to a continuum of the emitted particles. The energy spectra of the emitted particles provide information regarding nuclear level densities. The statistical models have been developed and reviewed comprehensively by a number of authors.[1–4] Bodansky[5] has reviewed the interpretation of the various experimental results in the light of the statistical models in compound-nuclear reactions.

In the present work, the neutron interaction of 14.8-MeV neutrons with 20 elements, ranging in mass numbers from 9 to 208, was measured by means of the neutron time-of-flight technique. The distributions of inelastically scattered neutrons were obtained at 90° for Be, B, C, Mg, Si, Ti, V, Mn, Fe, Co, Ni, Cu, Se, Y, Mo, Cd, Sb, Ce, W, and Pb. Similar measurements have been made by a number of workers[6–18] in the incident-neutron-energy regions of 3–12 and 14 MeV. The present measurements supplement and augment the inelastic neutron data available for the study of reaction mechanisms and level densities.

For many medium and heavy nuclei, the observed inelastically scattered spectra of 14.8-MeV neutrons are complicated by the presence of secondary neutrons emitted in the $(n, 2n)$ process. In all such cases, the distributions of the "first" neutrons have been obtained by means of the statistical-model formulation of Lang and Le Couteur.[19] The calculated inelastic distributions for the emission of the first neutrons have been used to obtain the level-density parameters based on a Fermi-gas model. It will be seen in the following sections that the level-density parameters obtained in this work follow the expected shell-model effects, specifically for the element Pb. These shell-model effects are justified on a theoretical basis by the consideration of the effect of shell closure upon the densities of single-particle orbits near the Fermi level in the nucleon gas.

The experimental procedures employed in the present measurements are described in Sec. II. The analytic procedures and the results are discussed in detail in Sec. III.

II. EXPERIMENTAL PROCEDURES

The experimental equipment used in the present measurements has been described in detail elsewhere.[20] Therefore, only a brief description of the experimental procedures is given here.

A source of 14.8-MeV neutrons was provided by

† Work supported in part by the U.S. Army Nuclear Defense Laboratory, Edgewood Arsenal, Md.
* Present address: Lowell Technological Institute, Lowell, Mass.
‡ Present address: University of Texas, Austin, Tex.
[1] J. Blatt and V. F. Weisskopf, *Theoretical Nuclear Physics* (John Wiley & Sons, Inc., New York, 1952).
[2] K. J. Le Couteur, in *Nuclear Reactions*, edited by P. M. Endt and M. Demur (North-Holland Publishing Co., Amsterdam, 1959).
[3] H. Feshbach, in *Nuclear Spectroscopy*, edited by F. Ajzenberg-Selove (Academic Press Inc., New York, 1969), Part B.
[4] T. Ericson, Advan. Phys. **9**, 425 (1960).
[5] D. Bodansky, in *Annual Review of Nuclear Science*, edited by E. Segré (Annual Reviews, Inc., Palo Alto, Calif., 1962).
[6] C. H. Holbrow and H. H. Barschall, Nucl. Phys. **42**, 264 (1963).
[7] D. B. Thomson, Phys. Rev. **129**, 1649 (1963).
[8] R. L. Clarke and W. G. Cross, Nucl. Phys. **53**, 177 (1964).
[9] S. G. Buccino, C. E. Hollandsworth, H. W. Lewis, and P. R. Bevington, Nucl. Phys. **60**, 17 (1964).
[10] R. M. Wilenzick, K. K. Seth, P. R. Bevington, and H. W. Lewis, Nucl. Phys. **62**, 511 (1965).
[11] G. A. Petitt, S. G. Buccino, and C. E. Hollandsworth, Nucl. Phys. **79**, 231 (1966).
[12] K. Tsukada, S. Tanaka, M. Maruyama, and Y. Tomita, Nucl. Phys. **78**, 369 (1966).
[13] L. Rosen and L. Stewart, Phys. Rev. **107**, 824 (1957).
[14] P. Huber, R. Plattner, C. Poppelbaum, and R. Wagner, Phys. Letters **5**, 202 (1963).
[15] K. K. Seth, R. M. Wilenzick, and T. A. Griffy, Phys. Letters **11**, 308 (1964).
[16] P. W. Martin, D. T. Stewart, and J. Martin, Nucl. Phys. **61**, 524 (1965).
[17] R. M. Schectman and J. D. Anderson, Nucl. Phys. **77**, 241 (1966).
[18] J. T. Prud'homme, I. L. Morgan, J. H. McCrary, J. B. Ashe, and O. M. Hudson, Jr., Texas Nuclear Corporation Report No. AFSWC-TR-60-30, 1960 (unpublished).
[19] J. M. B. Lang and K. J. Le Couteur, Proc. Phys. Soc. (London) **A67**, 586 (1954).
[20] S. C. Mathur, P. S. Buchanan, and I. L. Morgan, Texas Nuclear Corporation Report No. NDL-TR-86, 1967 (unpublished).

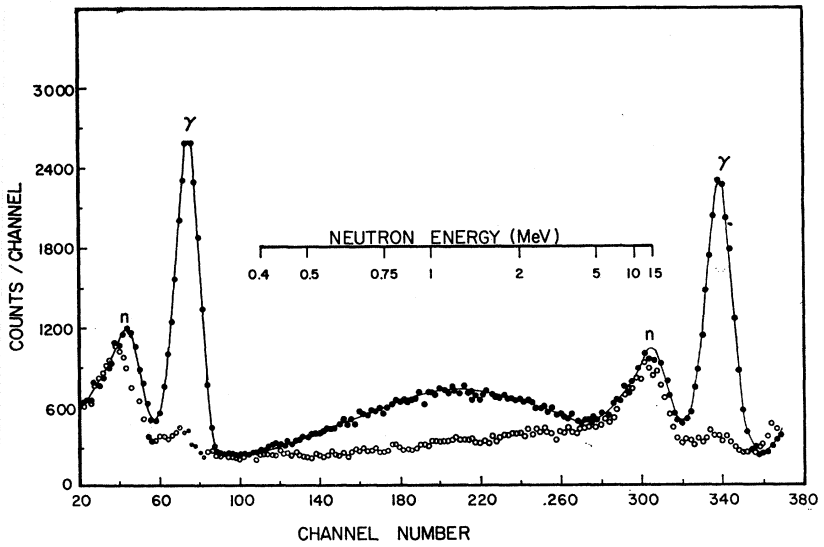

FIG. 1. Time-of-flight spectra for 14.8-MeV neutrons at 90° to the incident beam direction. The solid circles represent the spectrum for neutrons scattered by W. The open circles represent the spectrum with the scatterer removed.

Texas Nuclear Corp.'s 3.2-MeV Van de Graaff accelerator by means of the $T(d, n)\mathrm{He}^3$ reaction. The spectrum of scattered neutrons was recorded by a pulsed-beam time-of-flight spectrometer. The pulsed beam was obtained by sweeping the deuteron beam by means of an rf voltage of 2.54 MHz applied to a pair of electrostatic deflection plates located at the end of the accelerating column. A pair of adjustable chopping slits provided bursts of deuterons of 2- to 3-nsec duration.

The scattered neutrons were detected by means of a plastic scintillator 5.1 cm in diam and 5.1 cm in length, optically coupled to an RCA 6342 photomultiplier tube. The neutron detector was shielded by a cylindrical lead shell, 5.1 cm in thickness, surrounded by a mixture of lithium carbonate and paraffin. A 40-cm-long iron attenuator provided additional shielding from the direct neutron beam.

The scattering samples in this experiment were in the form of solid cylinders, 2.54 cm in diam and 5.1 cm in length, with the exception of B, B^{10}, C, Si, and Ce. The B and B^{10} samples were powders tightly packed into thin plastic containers, 4.0 cm in diam and 6.0 cm in length. The C scatterer was in the form of a hollow cylinder, with 2.54 cm o.d., 1.27 cm i.d., and 5.1 cm in length. The Si scatterer was in the form of powder tightly packed in a cylindrical plastic container, 2.54 cm in diam and 5.1 cm in length. The Ce scatterer was in the form of a solid cylinder, 2.0 cm in diam and 3.1 cm in length.

In the course of each data run, the neutron flux was continuously monitored by means of a calibrated long counter of the Hanson-McKibben[21] type. The long counter was set at 90° with respect to the incident deuteron beam direction and at a distance of 150 cm

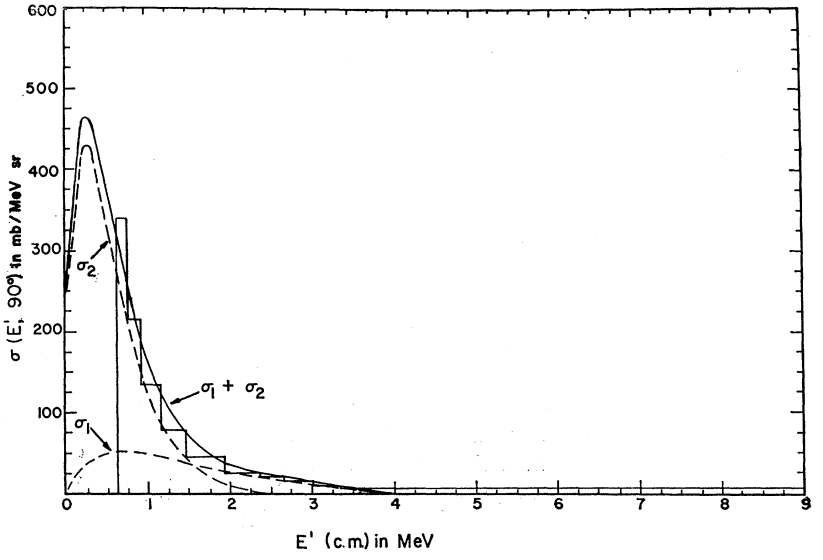

FIG. 2. Energy distribution of inelastic neutrons as a function of emitted-neutron energy for W. The histogram represents the experimental cross sections. The curves labelled σ_1 and σ_2 are the calculated distribution for the first and second neutrons, respectively. The curve labelled $\sigma_1+\sigma_2$ is the composite theoretical distribution.

[21] A. O. Hanson and J. L. McKibben, Phys. Rev. 72, 673 (1947).

TABLE I. Differential cross sections for neutron emission at 90° following neutron bombardment of several elements.

Element	E' (MeV)	$\sigma(E', 90°)$ (mb/sr)±20% 0–0.75[a]	0.75–7.0	Total
Be			31.88	31.88
B^{10}			112.16	112.16
B^{nat}			28.51	28.51
C			31.18	31.18
Mg		6.60	40.71	47.31
Si		31.40	41.88	73.28
Ti		48.81	78.43	127.24
V		54.31	97.56	151.87
Mn		56.41	97.84	154.25
Fe		44.77	76.01	120.78
Co		54.95	102.00	156.95
Ni		51.60	68.51	120.11
Cu		56.05	103.79	159.84
Se		119.03	108.50	227.53
Y		124.12	122.49	246.61
Mo		92.95	117.90	210.85
Cd		151.37	137.73	289.10
Sb		136.77	131.64	268.41
Ce		154.10	173.14	327.24
W		271.53	148.61	420.14
Pb		102.24	259.87	362.11

[a] The cross sections for the neutron energy range 0–0.75 MeV were not accessible directly from the experimental data, but instead were derived from theoretical calculations. See the discussion of this point in Sec. III A.

from the center of the tritium target to the front face of the long counter. The charge collected at the target cell was integrated simultaneously. All the data runs were made for a constant integrated charge. The mean energy of the incident neutrons was 14.8 MeV with an energy spread of approximately 0.1 MeV. The absolute flux calibration of the long counter was obtained with a proton recoil telescope.

A typical time-of-flight spectrum of emitted neutrons by W is shown in Fig. 1. A flight path of 150 cm was used throughout in this experiment. The resolution of the time-of-flight spectrometer was of the order of 7–10 nsec in the various runs.

In order to obtain the differential cross sections for the neutron emission, the time-of-flight spectrum was converted into an energy spectrum. The differential cross section for inelastic scattering at 90°, $\sigma(E', 90°)$, was calculated as an average over groups of channels commensurate with the resolution of the time-of-flight spectrometer. The details of the analysis are provided elsewhere.[20] The energy distributions of the emitted neutrons have been plotted as histograms of $\sigma(E', 90°)$, in units of mb/sr MeV, as a function of emitted neutron energy E'. Figure 2 shows the energy distribution of emitted neutrons for W. The cross sections $\sigma(E', 90°)$ for other elements obtained in the present experiment are presented in detail in graphical as well as tabular form elsewhere.[20] The neutron-emission cross sections at 90° for the elements investigated, summed over the outgoing-neutron-energy range, are presented in Table I.

The various sources of experimental uncertainties in obtaining and analyzing the spectral data are cumulative. The cumulated errors in the magnitude of the differential cross sections range from 17 to 25% in various energy regions.[20] A correction for neutron multiple scattering was applied in the analysis of the present data by means of the computer program MULTSCAT.[20]

III. RESULTS AND DISCUSSION

A. Energy Distribution of Emitted Neutrons

The energy distribution of emitted neutrons from W at 90° is shown in Fig. 2 in the form of a histogram of $\sigma(E', 90°)$ as a function of emitted-neutron energy E'. From the spectral data obtained in this experiment, similar energy distributions have been obtained for Be, B, C, Mg, Si, Ti, V, Mn, Fe, Co, Ni, Cu, Se, Y, Mo, Cd, Sb, Ce, and Pb at an angle of 90°. All of these distributions have been presented elsewhere.[20]

It can be seen from Fig. 2 that the cross-section data below an emitted-neutron energy of 0.6 MeV are unavailable. Because of the detector bias, the analysis is not reliable below this energy. To obtain the total cross sections for emitted neutrons over the entire energy region, it is therefore necessary to resort to theoretical calculations. The application of the compound-nucleus statistical model for the analysis of the present spectral data is described in the following. Similar analyses were performed by Rosen and Stewart[13] and by Huber *et al.*[14] for their inelastic neutron-scattering data obtained in the region of 14 MeV. The differential cross sections for neutron emission at 90° for the elements investigated, summed over the entire outgoing neutron-energy range, are presented in Table I. In addition, this Table provides a breakdown of the cross section into two energy regions, $E'=0$–0.75 MeV,

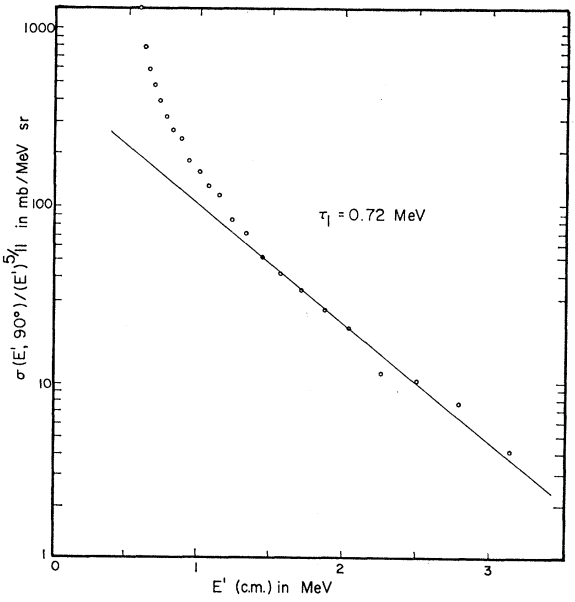

FIG. 3. Semilog plot of $\sigma(E', 90°)/(E')^{5/11}$ as a function of emitted-neutron energy E' for W. The straight-line portion of the plot provides the nuclear temperature τ_1 associated with the emission of the first neutron.

based on the theoretical considerations described below, and $E'=0.75$–7.0 MeV, obtained directly from the experimental data.

In the incident-neutron-energy region of 14.8 MeV, the $(n, 2n)$ process is energetically possible for most of the elements measured in the present experiment and competes effectively with the (n, n') process. The distribution obtained for W (Fig. 2) is typical of the cases where the emission of two neutrons in succession is an important process. In such cases, it is possible to obtain the distributions for the (n, n') and the $(n, 2n)$ processes separately by the application of the statistical-model formulation of Lang and Le Couteur.[2,19]

According to the formulation of Lang and Le Couteur, the nuclear temperature τ_1 associated with the emission of the first neutron can be obtained from the relation

$$\sigma(E)dE \propto E^{5/11} \exp(-12E/11\tau_1)dE. \quad (1)$$

For each spectrum, a semilog plot of $\sigma(E', \theta)/(E')^{5/11}$ as a function of scattered neutron energy E' was plotted. Figure 3 shows the plot for the W distribution. The slope of the straight-line portion of this plot is equal to $-\frac{12}{11}\tau_1$, providing the value of the nuclear temperature τ_1.

The energy distribution of the first neutron was then obtained by means of the statistical-model relation

$$\sigma(E')dE'=K_1E' \exp(-E'/\tau_1)dE', \quad (2)$$

where K_1 is the normalization constant.

The constant K_1 associated with the first neutron emission has been evaluated on the assumption that neutron emission, where energetically possible, is the predominant mode of decay, to the exclusion of γ emission. Hence, the first neutron distribution is assumed to be normalized to one half the emission cross section from zero to an energy

$$E_2=E_0-(B_n+0.5) \quad (3)$$

where E_0 is the incident neutron energy, and B_n is the neutron binding energy in MeV.

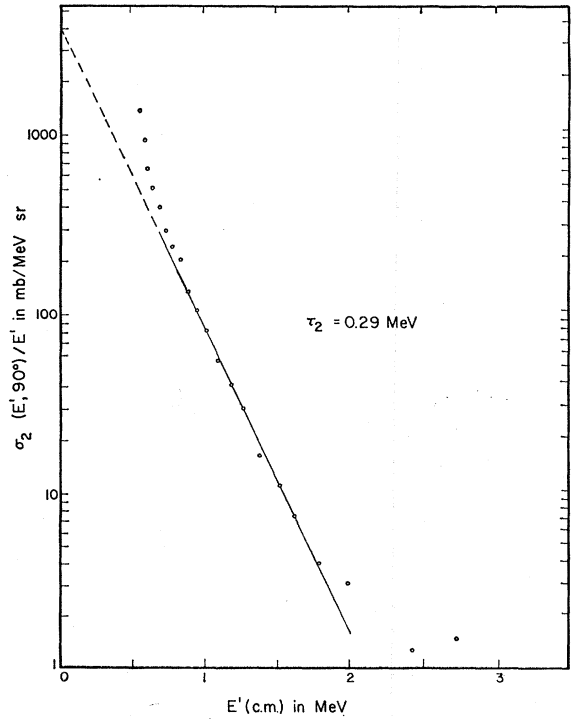

FIG. 4. Semilog plot of $\sigma_2(E', 90°)/E'$ as a function of E'. The straight-line portion of the plot provides the nuclear temperature τ_2 associated with the emission of the second neutron.

TABLE II. The nuclear temperatures τ_1 and τ_2 corresponding to the emission of the first and second neutrons, respectively.[a]

Element	Huber *et al.*[b] $\theta_{lab}=45°$ τ_1 (MeV)	Present work $\theta_{lab}=90°$ τ_1 (MeV)	τ_2 (MeV)
Mg		0.85	
Ti		1.08	0.39
V		1.08	0.43
Mn		1.01	0.41
Fe		1.18	0.38
Co		1.06	0.40
Ni		1.30	0.29
Cu		1.26	0.41
Se		0.94	0.32
Y		0.93	0.32
Mo	0.90	1.02	0.37
Cd	0.85	0.85	0.32
Sb	0.89	0.84	0.33
Ce	0.90	0.85	0.35
W		0.72	0.29
Pb	1.28	1.04	0.58

[a] The errors in the values of τ_1 and τ_2 obtained in this work have been estimated to be of the order of $\pm 10\%$.
[b] See Ref. 14.

In the actual analysis of the spectral data, it was noted that the experimental cross sections below the outgoing neutron energy of about 0.75 MeV are not reliable. In order to circumvent this difficulty, the right-hand side of Eq. (2) was integrated from an energy $E_1=0.75$ MeV to E_2, and the result equated to one-half of the experimentally determined emission cross section in this energy range. This procedure gives

$$\tfrac{1}{2}\sigma(E_1, E_2)=-K_1\tau_1[(E_1+\tau_1) \times \exp(-E_1/\tau_1)-(E_2+\tau_1) \exp(-E_2/\tau_1)], \quad (4)$$

where $\sigma(E_1, E_2)$ represents the integrated cross section between the energies E_1 and E_2. The normalization constant K_1 has been evaluated from Eq. (4). The neutron binding energies B_n were obtained from Seeger's[22] tables.

The theoretical distribution $\sigma_1(E')$ for the emission of the first neutron has been obtained by means of Eq. (2) with the use of parameters K_1 and τ_1. This distribution has been labelled σ_1 in Fig. 2.

In order to obtain the nuclear temperature τ_2 for the emission of the second neutron, the calculated distribution $\sigma_1(E')$ was subtracted from the experimental composite spectrum. The resulting distribution $\sigma_2'(E')$ is assumed to correspond to the emission of the second neutron. The nuclear temperature τ_2 corresponding to

[22] P. A. Seeger, Nucl. Phys. 25, 1 (1961).

TABLE III. Calculated Fermi-gas level-density coefficients.

Element	a (MeV^{-1}) Present experiment	Huber *et al.*[a]	Seth *et al.*[b]
Mg	11.4		
Ti	8.0		
V	9.3		
Mn	11.0		
Fe	7.5		2.4
Co	9.8		
Ni	6.2		
Cu	6.7		
Se	11.3		
Y	13.3		10.9
Mo	10.2	13.5	
Cd	14.8	14.9	15.9
Sb	16.6	14.8	
Ce	15.5	14.2	
W	21.7		23.8
Pb	10.7	6.6	11.0

[a] See Ref. 14.
[b] See Ref. 15.

the emission of the second neutron was obtained from a semilog plot of $\sigma_2'(E')/E'$ as a function of outgoing neutron energy E'. The plot for the W distribution is shown in Fig. 4. The slope of the straight-line portion of this plot gives the nuclear temperature τ_2, and the intercept of the ordinate, the normalization factor K_2. A new distribution $\sigma_2(E')$ for the emission of the second neutron was then calculated by means of Eq. (2), using the parameters K_2 and τ_2. The calculated distributions σ_1, σ_2, and $\sigma_1+\sigma_2$ are shown in Fig. 2.

The nuclear temperatures τ_1 and τ_2 obtained for various elements in this experiment are presented in Table II. This analysis has not been performed for Be, B, C, and Si, since the statistical model is not applicable in the region of low-mass numbers.

In the case of the Mg spectrum, the contribution due to the $(n, 2n)$ process is expected to be insignificant. In obtaining the nuclear temperatures associated with these distributions, it was assumed, therefore, that the entire contribution was due to the (n, n') process.

Table II also lists the nuclear temperatures τ_1 obtained by Huber *et al.*[14] for Mo, Cd, Sb, Ce, and Pb for the distribution of inelastically scattered neutrons at an angle of 45°, with the incident neutron energies equal to 14 MeV. The agreement between these results and the present measurements is, in general, good.

It may be noted here that the present analysis has been made under the assumption that the neutron emission, where energetically possible, has essentially unit probability in competition with the γ emission. Recently, however, Cohen *et al.*[23] have shown by coincidence studies of $(p, p'n)$ and $(p, p'\gamma)$ reactions on Sn^{119} and Ni^{61} that this assumption may not be universally valid. These departures from the basic assumption should be incorporated in the analyses of the neutron energy spectra when quantitative estimates of the relative probabilities for the emission of the neutron and the γ ray are available in the future.

B. Level-Density Coefficients

In the nuclear reactions where the compound-nucleus formation is the dominant mechanism, the spectra of the emitted particles contain information regarding the nuclear-level density. The shape of the evaporation spectrum is given by an expression of the form

$$\sigma(E')dE' \propto \sigma_{\text{inv}}^*(E')\rho(U)dE', \tag{5}$$

where σ_{inv}^* is the cross section for the formation of the compound nucleus by the emitted particle incident on the residual nucleus with an energy E', and $\rho(U)$ is the level density at excitation U.

A variety of functional forms have been proposed for the level density $\rho(U)$, based on the description of a nucleus as a Fermi gas. A simple expression which fits the experimental data satisfactorily, in general, is given by

$$\rho(U) = a \exp(-E'/\tau), \tag{6}$$

where a is the Fermi-level density coefficient, and τ is the nuclear temperature. The Fermi-gas model provides the relation between a and τ as

$$a = E_{\text{eff}}/\tau^2, \tag{7}$$

where

$$E_{\text{eff}} = E_0 - 2\tau + P(Z) + P(N). \tag{8}$$

The $P(Z)$ and $P(N)$ are the pairing energy corrections.[24] The E_0 is the incident particle energy.

In the present experiment, the level-density coefficients have been calculated with the use of nuclear temperatures τ_1 associated with the emission of the first neutron. The pairing energy corrections $P(N)$ for neutrons were obtained by averaging over the various isotopic contents of each of the natural elements used as scatterers.

The calculated values of the level-density coefficients are listed in Table III. The results of Seth *et al.*[15] and of Huber *et al.*[14] obtained in the incident-neutron-energy regions of 6 and 14 MeV, respectively, are also tabulated for comparison.

It can be seen from Table III that there is good agreement between the three sets of level-density coefficients. There is a large discrepancy between the present value of a for Fe and the one obtained by Seth *et al.*[15] However, the agreement for Y, Cd, W, and Pb is gratifying, particularly since at 14.8-MeV neutron energy, there is the added complexity in the spectra due to the emission of two neutrons in succession. The

[23] B. L. Cohen, E. C. May, T. M. O'Keefe, C. L. Fink, and B. Rosner, Phys. Rev. Letters **21**, 226 (1968).

[24] A. G. W. Cameron, Can. J. Phys. **36**, 1040 (1958).

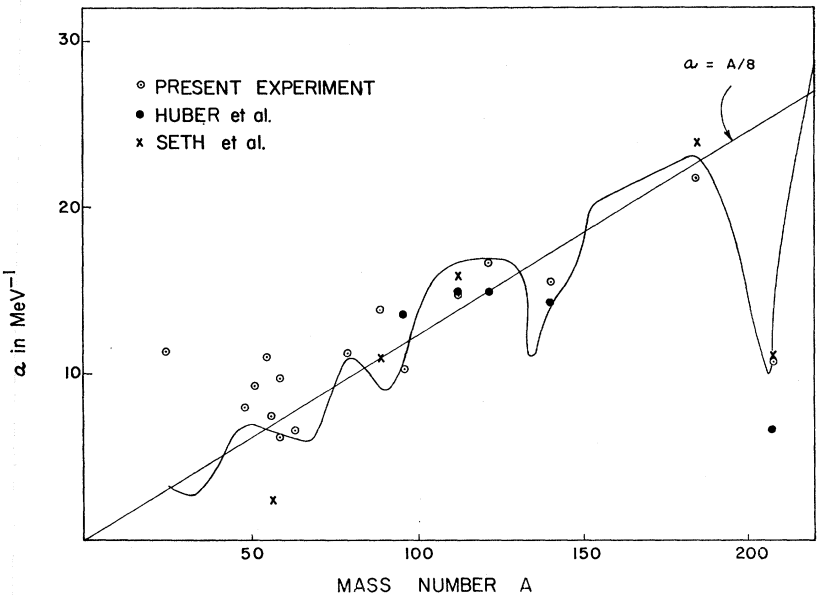

FIG. 5. Plot of calculated level-density coefficients as a function of mass number. The three sets of data points represent the results of the present experiment, and those of Huber *et al.* (Ref. 14) and Seth *et al.* (Ref. 15). The solid curve represents the shell-model calculations based on the formulation of Newton as modified by Lang. The straight line represents an empirical fit to the data, with $a=A/8$, where A is the mass number of the element.

good agreement at two different incident energies may be interpreted as a test of the self-consistency of level-density coefficients.

The calculated level-density coefficients have also been plotted in Fig. 5 as a function of mass number A. The curved line represents the theoretical calculations of Newton[25] as modified by Lang.[26] These calculations take into account the effects of shell closure upon the densities of single-particle orbits. The straight line represents an empirical fit to the experimental results. Such a fit is shown in the review article by Bodansky.[5]

It may be pointed out that the present results agree with the expected dip in the level-density coefficients near the doubly-closed-shell structure of Pb^{208}. It can be concluded from an examination of Fig. 5 that, in general, the present results are in good agreement with the predictions of the shell-model calculations.[25,26]

IV. SUMMARY

In the present work, the spectra of emitted scattered neutrons have been measured for 20 elements by means of the neutron time-of-flight technique. The spectral data have been reduced to emission cross sections, and the spectral shapes have been fitted by the compound-nuclear statistical model, except for the light elements. The spectral data have been presented both in the graphical as well as in the tabular form elsewhere.[20] It has been found that for medium-weight and heavy nuclei, the predominant reaction mechanism follows the general predictions of the statistical model.

At an incident neutron energy of 14.8 MeV, the emission of a successive neutron by the $(n, 2n)$ process is quite significant. In the present analysis, the neutron distributions for the emission of the first and second neutrons have been obtained by the application of the formulation of Lang and Le Couteur.[19] The nuclear temperatures associated with the emission of the first neutron have been used to obtain Fermi level-density coefficients. The present results are, in general, in good agreement with the predictions of the shell-model calculations and the experimental results of other workers.

ACKNOWLEDGMENTS

The authors wish to express their appreciation to D. O. Nellis, J. B. Ashe, and J. D. Hall for their assistance in the time-of-flight experiments. Thanks are also due to Robert Sieberg for performing very patiently the tedious task of reducing the spectral data to cross sections.

[25] T. D. Newton, Can. J. Phys. **34**, 804 (1956).
[26] D. W. Lang, Nucl. Phys. **26**, 434 (1961).